

On the Numerical Evaluation of One-Loop Amplitudes: the Gluonic Case

W. T. Giele*

Fermilab, Batavia, IL 60510, USA

G. Zanderighi†

The Rudolf Peierls Centre for Theoretical Physics, 1 Keble Road, University of Oxford, UK.

ABSTRACT: We develop an algorithm of polynomial complexity for evaluating one-loop amplitudes with an arbitrary number of external particles. The algorithm is implemented in the **Rocket** program. Starting from particle vertices given by Feynman rules, tree amplitudes are constructed using recursive relations. The tree amplitudes are then used to build one-loop amplitudes using an integer dimension on-shell cut method. As a first application we considered only three and four gluon vertices calculating the pure gluonic one-loop amplitudes for arbitrary external helicity or polarization states. We compare our numerical results to analytical results in the literature, analyze the time behavior of the algorithm and the accuracy of the results, and give explicit results for fixed phase space points for up to twenty external gluons.

KEYWORDS: QCD, NLO Computations, Jets, Hadronic Colliders.

*email: giele@fnal.gov

†email: g.zanderighi1@physics.ox.ac.uk

Contents

1. Introduction	1
2. Construction of the Algorithm	3
3. Results	6
3.1 Checks of the Results	6
3.2 Study of the Accuracy	7
3.3 Time Dependence of the Algorithm	10
3.4 Results for fixed phase space points	11
4. Conclusions and outlook	13
A. More numerical results	15

1. Introduction

The current Tevatron collider and the upcoming Large Hadron Collider (LHC) experiments require a good understanding of the Standard Model signals to carry out a successful search for the Higgs particle and physics beyond the Standard Model. At these hadron colliders QCD plays an essential role and modeling all of the aspects of the events is crucial. From the lessons learned at the Tevatron, we need fixed order calculations matched with parton shower Monte Carlo's and hadronization models for a successful understanding of the observed events.

Fixed order calculations are the first step in modeling the events. In this paper we describe an algorithm for the automated calculation of one-loop amplitudes. A successful implementation of numerical algorithms for evaluating fixed order amplitudes needs to take into account the so-called complexity of the algorithm. That is, how does the evaluation time grow with the number of external particles. An algorithm of polynomial complexity is highly desirable [1]. Another consideration is the suitability of the method within a numerical context. In particular algebraic methods can be successfully implemented in efficient and robust algorithms. This can lead to rather different methods from what one would develop and use in analytic calculations.

Leading order parton level generators are well understood. These have been constructed using algebraic manipulation programs to calculate the tree amplitudes directly from Feynman diagrams [2–6]. However, such a direct approach leads to algorithms of double factorial complexity. Techniques such as helicity amplitudes [7–10], color ordering [11, 12] and recursion relations [13–17] have been developed and successfully used both

in analytic and numerical calculations of leading order amplitudes. These techniques all aim at further factorizing the calculation in smaller subsets. Of these the recursion relation technique stands out as it maximizes the factorizability of tree amplitudes and consequently can be implemented as a polynomial complexity algorithm of rank four [18]. Furthermore, recursion relations have a simple algebraic structure ideal for numerical evaluation of the tree amplitudes. Such a recursive algorithm was successfully implemented in tree amplitude generators [19, 20].

Compared to leading order generators the status of next-to-leading order generators is far less advanced. Calculations based on explicit one-loop Feynman diagrams using tensor form factor reductions have been used successfully for four, five and six point amplitudes. Examples of recent explicit calculations of six point one-loop amplitudes using such brute force methods are six photons [21, 22], six gluons [23] and $e^+e^- \rightarrow$ four fermions [24, 25]. These direct approaches suffer from worse than factorial complexity.

Alternatively, powerful analytic methods have been developed for one-loop amplitudes based on generalized unitarity methods [26–45]. These methods have been used in analytic calculations leading to compact expressions for processes such as for example vector boson plus four partons [46, 47]. The analytic methods developed are again based on the principle of factorization. By using generalized unitarity one can factorize the one-loop amplitude into tree amplitudes from which the coefficients of the master integrals can be constructed.

The main problems of converting the on-shell analytic method into numerical algorithms are twofold. The first issue is resolving overlapping contributions between quadruple, triple and double cuts. Using the methods developed in [48, 49] one can disentangle the contributions in an algebraic manner. Secondly, the numerical implementation of the dimensional regularization within an on-shell method leads to complications. The on-shell cut lines give intermediate on-shell particles in non-integer number of dimensions. These lines are ill-defined and require special considerations. In particular from the aspect of a numerical implementation one needs a well-defined method for calculating the contributions originating from dimensional regularization. Several methods to calculate these contributions applicable for numerical implementation have been developed [34, 35, 50–52]. These developments now allow the construction of numerical algorithms for evaluating one-loop amplitudes with a large number of external particles [53, 54].

In this paper we present an algorithm of rank nine polynomial complexity to calculate one-loop amplitudes with an arbitrary number of particles based on the purely algebraic methods developed in refs. [49, 51]. As a first step we implement the algorithm in the program **Rocket**¹ using three and four gluon vertices to calculate all the helicity amplitudes of the pure gluonic scattering amplitudes.

The outline of the paper is as follows. In section 2 we review the method and outline the construction of the required orthonormal basis vectors and D -dimensional polarization vectors. Section 3 contains our results: we study the accuracy of the method, the power-like growth of the computation time and give explicit single event results for various helicity configurations for up to twenty gluons. Finally, in section 4 we draw our conclusions and

¹From the Italian **Rucola**: **R**ecursive **U**nitariness **C**alculation of **O**ne-**L**oop **A**mplitudes.

give an outlook on our future plans.

2. Construction of the Algorithm

We implement the methods developed in refs. [49, 51] with some minor modifications into the **Rocket** program. These methods build upon the formalism of ref. [48] by removing the requirement of the four dimensional spinor language, thereby allowing for the extension of the method to D -dimensional cuts.

To calculate the full one-loop N -gluon amplitude, it is sufficient to be able to calculate the leading color ordered one-loop amplitude. From these color ordered amplitudes the full one-loop amplitude can be constructed [26, 55]. Eventually the one-loop amplitude has to be contracted with the tree amplitude, summed over the colors and integrated over phase space. The number of different orderings one needs to calculate can be drastically reduced by noting that the phase space integration will symmetrize the final state gluons. Alternatively, a more physical approach can be employed by not only randomly sampling over the helicities but also over the colors of the external gluons. In the following we will therefore focus on the leading color ordered amplitudes $A_N^{[1]}(1, 2, \dots, N)$.

We will use the master integral basis decomposition derived in ref. [51]. This decomposition in an overcomplete set of master integrals makes the loop momentum dependence on the dimensionality explicit:

$$\begin{aligned}
A_N^{[1]} = & - \sum_{[i_1|i_5]} \frac{(D-4)}{2} e_{i_1 i_2 i_3 i_4 i_5}^{(2,0)} I_{i_1 i_2 i_3 i_4 i_5}^{(D+2)} \\
& + \sum_{[i_1|i_4]} \left(d_{i_1 i_2 i_3 i_4}^{(0,0)} I_{i_1 i_2 i_3 i_4}^{(D)} - \frac{(D-4)}{2} d_{i_1 i_2 i_3 i_4}^{(2,0)} I_{i_1 i_2 i_3 i_4}^{(D+2)} + \frac{(D-4)(D-2)}{4} d_{i_1 i_2 i_3 i_4}^{(4,0)} I_{i_1 i_2 i_3 i_4}^{(D+4)} \right) \\
& + \sum_{[i_1|i_3]} \left(c_{i_1 i_2 i_3}^{(0,0)} I_{i_1 i_2 i_3}^{(D)} - \frac{(D-4)}{2} c_{i_1 i_2 i_3}^{(2,0)} I_{i_1 i_2 i_3}^{(D+2)} \right) \\
& + \sum_{[i_1|i_2]} \left(b_{i_1 i_2}^{(0,0)} I_{i_1 i_2}^{(D)} - \frac{(D-4)}{2} b_{i_1 i_2}^{(2,0)} I_{i_1 i_2}^{(D+2)} \right), \tag{2.1}
\end{aligned}$$

where we introduced the short-hand notation $[i_1|i_n] = 1 \leq i_1 < i_2 < \dots < i_n \leq N$ and

$$I_{i_1, \dots, i_N}^D = \int \frac{d^D l}{i\pi^{D/2}} \frac{1}{d_{i_1} d_{i_2} \dots d_{i_N}}, \tag{2.2}$$

with $d_i = d_i(l) = (l+q_i)^2 = (l+p_1+\dots+p_i)^2$. In this basis the coefficients $b_{i_1 i_2}^{(0,0)}$, $b_{i_1 i_2}^{(2,0)}$, $c_{i_1 i_2 i_3}^{(0,0)}$, $c_{i_1 i_2 i_3}^{(2,0)}$, $d_{i_1 i_2 i_3 i_4}^{(0,0)}$, $d_{i_1 i_2 i_3 i_4}^{(2,0)}$, $d_{i_1 i_2 i_3 i_4}^{(4,0)}$, and $e_{i_1 i_2 i_3 i_4 i_5}^{(2,0)}$ are independent of the loop momentum dimensionality D . Because the coefficients $d_{i_1 i_2 i_3 i_4}^{(4,0)}$, $c_{i_1 i_2 i_3}^{(2,0)}$ and $b_{i_1 i_2}^{(2,0)}$ are multiplied with a dimensional factor $(D-4)$ they cannot be determined using four dimensional cuts². Therefore we need to extend the dimensionality of the cut line to higher dimensions. We choose the dimensionality to be an integer, resulting in a well defined on-shell particle after performing the cut [51].

²Note that the terms proportional to $e_{i_1 i_2 i_3 i_4 i_5}^{(2,0)}$ and $d_{i_1 i_2 i_3 i_4}^{(2,0)}$ will contribute only at $\mathcal{O}(\epsilon)$.

By applying quintuple, quadruple, triple and double D_s -dimensional cuts (where $D_s \geq D$ denotes the dimensionality of the spin-space) we can determine the coefficients of the parametric form of the one-loop amplitude. This requires the calculation of the factorized un-integrated one-loop amplitude

$$\begin{aligned} \text{Res}_{i_1 \dots i_M}(\mathcal{A}_N^{[1]}(l)) &= \left(d_{i_1} \times \dots \times d_{i_M} \times \mathcal{A}_N^{[1]}(l) \right)_{d_{i_1} = \dots = d_{i_M} = 0} \\ &= \sum_{\{\lambda_1, \dots, \lambda_M\}=1}^{D_s-2} \left(\prod_{k=1}^M \mathcal{A}_{i_{k+1}-i_k}^{[0]}(l_{i_k}^{(\lambda_k)}, p_{i_k+1}, \dots, p_{i_{k+1}}, -l_{i_{k+1}}^{(\lambda_{k+1})}) \right), \end{aligned} \quad (2.3)$$

where $M \leq 5$ and the D -dimensional loop momentum l has to be chosen such that $d_{i_1}(l) = \dots = d_{i_M}(l) = 0$. As a result of the on-shell condition, the tree amplitudes $\mathcal{A}^{[0]}$ have in addition to the external four dimensional gluons, two D_s -dimensional gluons with complex momenta. Dimensional regularization requires that $D_s \geq D$ such that the ultra-violet poles are regulated. These higher dimensional gluons have $(D_s - 2)$ polarization states. To calculate these tree amplitudes we use the standard Berends-Giele recursion relation [13] which is valid in arbitrary dimension and for complex momenta.

The generic solution for the loop momentum in eq. (2.3) is given by

$$l_{i_1 \dots i_M}^\mu = V_{i_1 \dots i_M}^\mu + \sqrt{\frac{-V_{i_1 \dots i_M}^2}{\alpha_M^2 + \dots + \alpha_D^2}} \left(\sum_{i=M}^D \alpha_i n_i^\mu \right), \quad (2.4)$$

for arbitrary values of the variables α_i .³

The vector $V_{i_1 \dots i_M}^\mu$ is defined in the space spanned by the denominator offset momenta $\{q_{i_1}, \dots, q_{i_M}\}$, while the orthonormal basis vectors $\{n_M^\mu, \dots, n_D^\mu\}$ span the space orthogonal to the space spanned by these momenta [49, 51]. Given the solution to the on-shell conditions $l_{i_1 \dots i_M}^\mu$ in eq. (2.4), the loop momenta flowing into the tree amplitudes l_{i_k} and $l_{i_{k+1}}$ in eq. (2.3) are fixed by momentum conservation (see ref. [49]).

Finally we need a stable and general method for constructing the orthonormal set of $(D - M)$ basis vectors and the $(D_s - 2)$ polarization vectors. To accomplish this we use the generalized Kronecker delta tensors [56] given by

$$\delta_{\nu_1 \nu_2 \dots \nu_R}^{\mu_1 \mu_2 \dots \mu_R} = \begin{vmatrix} \delta_{\nu_1}^{\mu_1} & \delta_{\nu_2}^{\mu_1} & \dots & \delta_{\nu_R}^{\mu_1} \\ \delta_{\nu_1}^{\mu_2} & \delta_{\nu_2}^{\mu_2} & \dots & \delta_{\nu_R}^{\mu_2} \\ \vdots & \vdots & & \vdots \\ \delta_{\nu_1}^{\mu_R} & \delta_{\nu_2}^{\mu_R} & \dots & \delta_{\nu_R}^{\mu_R} \end{vmatrix}. \quad (2.5)$$

We use the notation

$$\delta_{\nu_1 q \dots \nu_R}^{\mu_2 \dots \mu_R} \equiv \delta_{\nu_1 \nu_2 \dots \nu_R}^{\mu_1 \mu_2 \dots \mu_R} p_{\mu_1} q^{\nu_2}. \quad (2.6)$$

The $(R - 1)$ -particle Gram determinant is then given by

$$\Delta(k_1, k_2, \dots, k_{R-1}) = \delta_{k_1 k_2 \dots k_{R-1}}^{k_1 k_2 \dots k_{R-1}}. \quad (2.7)$$

³The conformal transformation applied on the coefficients α_i is only valid when $V_{i_1 \dots i_M}^2 \neq 0$. For the special case $V_{i_1 \dots i_M}^2 = 0$ a similar solution is found.

Note that for $R \geq D + 1$ the generalized Kronecker delta is zero. For the special case $R = D$ we have the factorization of the Kronecker delta into a product of Levi-Civita tensors: $\delta_{\nu_1 \nu_2 \dots \nu_D}^{\mu_1 \mu_2 \dots \mu_D} = \varepsilon^{\mu_1 \mu_2 \dots \mu_D} \varepsilon_{\nu_1 \nu_2 \dots \nu_D}$.

Given a set of momenta $\{q_1, q_2, \dots, q_M\}$ in a D -dimensional space-time we describe here how to construct the orthonormal set of basis vectors $\{n_1, \dots, n_{D-M}\}$ such that $q_i \cdot n_j = 0$ and $n_i \cdot n_j = \delta_{ij}$. The set of momenta span the M -dimensional sub-space. The basis vector set $\{n_i\}$ spans the orthogonal $(D - M)$ -dimensional space. For the k -th basis vector we choose the arbitrary vector b_k . The vector is then given by

$$n_k^\mu = \frac{\delta_{b_k b_{k-1} \dots b_1 q_1 \dots q_M}^\mu}{\sqrt{\Delta(b_{k-1}, \dots, b_1, q_1, \dots, q_M) \Delta(b_k, \dots, b_1, q_1, \dots, q_M)}}, \quad (2.8)$$

with $q_i \cdot n_k = 0$ and $n_j \cdot n_k = \delta_{jk}$. Note that arbitrary vector b_{D-M} in the basis vector n_{D-M}^μ drops out trivially because $\delta_{\mu_1 \dots \mu_D}^{\nu_1 \dots \nu_D} = \varepsilon_{\mu_1 \dots \mu_D} \times \varepsilon^{\nu_1 \dots \nu_D}$. This means that in the construction of the basis we used $(D - M - 1)$ arbitrary vectors.

We can also use the above construction of the orthonormal basis vectors to define the D_s -dimensional polarization states of the cut gluon lines. Given a D_s -dimensional gluon with light-cone momentum p we want to construct a set of the $(D_s - 2)$ polarization vectors $\{e_\mu^{(i)}\}$. The polarization vectors have the property $p \cdot e^{(i)} = 0$, $e^{(i)} \cdot e^{(j)} = -\delta_{ij}$ and the spin sum is

$$\sum_{i=1}^{D_s-2} e_\mu^{(i)} e_\nu^{(i)} = -g_{\mu\nu}^{(D_s)} + \frac{p_\mu v_\nu + p_\nu v_\mu}{p \cdot v} - \frac{p_\mu p_\nu v^2}{(p \cdot v)^2}, \quad (2.9)$$

where v_μ is the polarization gauge vector. Note that if v_μ is a light-cone vector the last term on the right-hand side is zero. The polarization vectors are easily constructed. We construct the $(D_s - 2)$ orthonormal basis vectors n_i^μ with respect to the two four-vectors $\{p, v\}$. We now define the $(D_s - 2)$ polarization vectors as $e_\mu^{(j)} = i n_{j\mu}$. Then $p \cdot e^{(i)} = 0$, $e^{(i)} \cdot e^{(j)} = -n_i \cdot n_j = -\delta_{ij}$, and eq. (2.9) is satisfied.

Once all coefficients in eq. (2.1) have been determined using an appropriate set of cuts and loop momentum solution vectors, we can algebraically continue the dimensionality to the non-integer limit: $D \rightarrow 4 - 2\epsilon$. This limit can be performed in different manners, leading to different schemes. In the four dimensional helicity scheme [57, 58] the continuation is defined as $D_s \rightarrow 4$, $D \rightarrow 4 - 2\epsilon$ while $D_s \geq D$. In the 't Hooft-Veltman scheme [59] the limit is defined as $D_s \rightarrow 4 - 2\epsilon$, $D \rightarrow 4 - 2\epsilon$ while $D_s \geq D$.

Because we are interested in the next-to-leading order contributions we can neglect terms of order ϵ in the continuation of the dimensionality. We then find for the color ordered one-loop amplitude

$$\begin{aligned} A_N^{[1]} &= \sum_{[i_1|i_4]} d_{i_1 i_2 i_3 i_4}^{(0,0)} I_{i_1 i_2 i_3 i_4}^{(4-2\epsilon)} + \sum_{[i_1|i_3]} c_{i_1 i_2 i_3}^{(0,0)} I_{i_1 i_2 i_3}^{(4-2\epsilon)} + \sum_{[i_1|i_2]} b_{i_1 i_2}^{(0,0)} I_{i_1 i_2}^{(4-2\epsilon)} \\ &- \sum_{[i_1|i_4]} \frac{d_{i_1 i_2 i_3 i_4}^{(4,0)}}{6} + \sum_{[i_1|i_3]} \frac{c_{i_1 i_2 i_3}^{(2,0)}}{2} - \sum_{[i_1|i_2]} \frac{(q_{i_1} - q_{i_2})^2}{6} b_{i_1 i_2}^{(2,0)} + \mathcal{O}(\epsilon). \end{aligned} \quad (2.10)$$

The terms in the first line give rise to the so-called cut-constructible part of the amplitude [60]. The terms in the second line can be identified with the rational part. In the approach used in this paper the division between these two contributions is not relevant.

For the numerical evaluation of the bubble, triangle and box master integrals we use the package developed in ref. [61].

3. Results

The algorithm is implemented in the **Rocket Fortran 95** program. We first perform a series of checks by comparing to existing analytic results in the literature and by performing internal consistency checks. Next the accuracy of the results up to eleven external gluons is examined by comparing to the analytically known one-loop N -gluon helicity amplitudes. We then show that the evaluation time as a function of the number of external gluons is consistent with a degree nine polynomial. Finally, we present explicit results for a few fixed phase space points for selected helicity configurations with up to twenty external gluons.

In next-to-leading order calculations, the external gluons of the one-loop amplitude are identified with the momenta of well-separated jets. We therefore impose the following set of cuts on the generated phase space momenta

$$|\eta_i| < 3, \quad p_{\perp,i} > 0.01\sqrt{s}, \quad R_{ij} = \sqrt{\phi_{ij}^2 + \eta_{ij}^2} > 0.4, \quad (3.1)$$

where η_i and $p_{\perp,i}$ denote the rapidity and transverse momentum of particle i , $\phi_{ij} = |\phi_i - \phi_j|$ and $\eta_{ij} = |\eta_i - \eta_j|$ denote the distance in azimuthal angle and rapidity between particle i and j and $s = (E_1 + E_2)^2$ is the center of mass collision energy squared.

The unrenormalized one-loop N -gluon results are given in the four dimensional helicity scheme (FDH). The conversion to the 't Hooft-Veltman (HV) scheme is given by

$$A_{\text{v,HV}} = A_{\text{v,FDH}}^v - \frac{c_{\Gamma}}{3} A_{\text{tree}}, \quad (3.2)$$

with

$$c_{\Gamma} = \frac{(4\pi)^{\epsilon}}{16\pi^2} \frac{\Gamma(1+\epsilon)\Gamma^2(1-\epsilon)}{\Gamma(1-2\epsilon)}. \quad (3.3)$$

We will give explicit results for double poles, single poles and the constant part after extraction of the factor c_{Γ} . The pole structure of the N -gluon one-loop amplitude is given by [62–64]

$$A_{\text{v,poles}} = c_{\Gamma} \left(-\frac{N}{\epsilon^2} + \frac{1}{\epsilon} \left(\sum_{i=1}^N \ln \left(\frac{-s_{i,i+1}}{\mu^2} \right) - \frac{11}{3} \right) \right) A_{\text{tree}}, \quad (3.4)$$

where as usual the indices are modulo N . For the dimensional scale μ we use the center of mass collision energy, $\mu^2 = s$.

3.1 Checks of the Results

We have performed several checks on our numerical implementation:

- we checked that the pole structure of the one-loop amplitudes agree with eq. (3.4) up to twenty gluons;

- the number of loop momentum solutions to the on-shell conditions in eq. (2.4) is infinite. This means we can solve for the coefficients in the parametric form of the integrand using many different sets of equations. We verified that the results are independent of the chosen loop momentum solutions;
- we checked that the results are independent of all auxiliary vectors introduced in e.g. eq. (2.8) used to construct both the orthonormal basis and the polarization vectors;
- we verified that our results are independent of the choice of dimensionality of the cut lines;
- for six gluons we compared all one-loop helicity amplitudes with the numerical results of [23];
- for up to twenty gluons we compared with the analytically known one-loop helicity amplitudes where all gluons have positive helicities [33, 65];
- for up to twenty gluons we compared with the analytically known one-loop helicity amplitudes where all but one gluon have positive helicities [33, 65];
- for up to twenty gluons we compared with the analytically known one-loop helicity amplitudes where all but two adjacent gluons have positive helicities [26, 60, 66].

All checks performed were successful.

3.2 Study of the Accuracy

To study the numerical accuracy of the on-shell method implemented in **Rocket** we define

$$\varepsilon_C = \log_{10} \frac{|A_N^{\text{v,unit}} - A_N^{\text{v,anly}}|}{|A_N^{\text{v,anly}}|}, \quad (3.5)$$

where “unit” denotes the result obtained with the on-shell method and “anly” the analytical result for the constant parts of the one-loop helicity amplitudes (or in the case of $N = 6$ the numerical results of [23]). Similarly, where relevant, we denote by ε_{DP} and ε_{SP} the accuracy on the double and single poles, respectively.

In fig. (1) we show the accuracy for the two adjacent minus helicity gluon MHV one-loop amplitudes, $A_N^{[1]}(- - + \cdots +)$, for N ranging between six and eleven. The 100,000 phase space points used for each multiplicity are generated uniformly in phase space using the Rambo algorithm [67]. We plot the accuracy for the double pole ($X = \text{DP}[\text{dp}]$, solid, red), the single pole ($X = \text{SP}[\text{dp}]$, green, dot-dashed) and the constant part ($X = \text{C}[\text{dp}]$, blue, dotted). We first examine the six-gluon plot (fig. (1), top left) and see that an excellent accuracy can be reached for all three contributions, the position of the peak being at $\varepsilon_{\text{DP}} = 10^{-12.8}$, $\varepsilon_{\text{SP}} = 10^{-11.6}$, and $\varepsilon_C = 10^{-10.8}$, respectively. The tail of the distribution reaching to large values of ε contains only a very few points for the single pole and the constant term. This lack of agreement is due to numerical instabilities. The well-known sources of instabilities are vanishing Gram determinants or other small intermediate

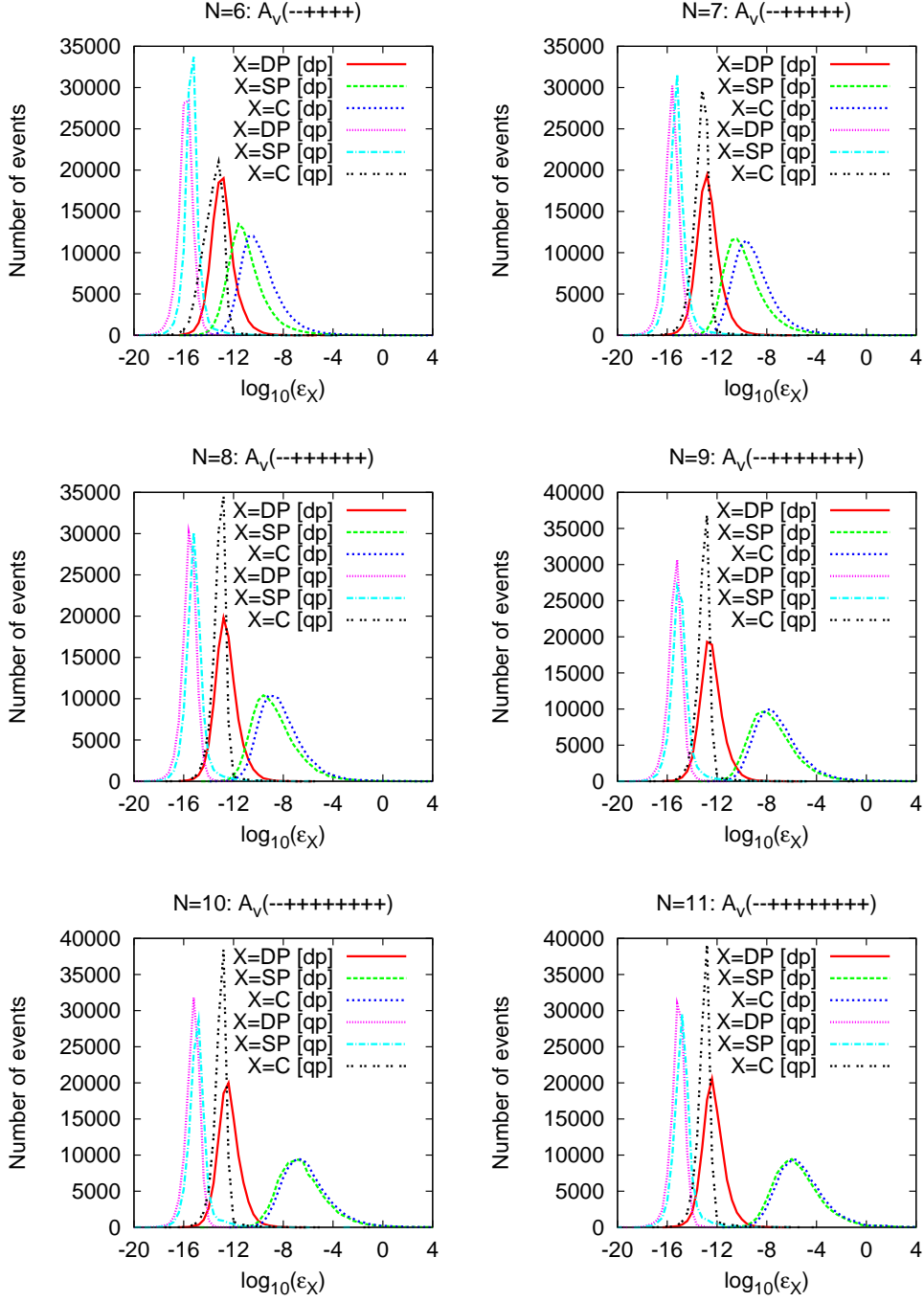


Figure 1: Accuracy on the double pole, single pole and constant part of the MHV amplitude with adjacent negative helicities for 6 up to 11 external gluons. Double ([dp]) and quadrupole ([qp]) precision results for 100,000 phase space points are shown. See text for more details.

denominators. Several techniques have been developed in the past to deal with such exceptional points, such as developing systematic expansions [68–70] or interpolating across

the singular regions [71]. Similarly to what is done in [5, 50, 54], we adopt here a more brute force approach and recur to quadrupole precision. In (fig. (1), top left) we see three more curves: they correspond to the numerical accuracy on the same 100,000 phase space points when the one-loop amplitude is computed in quadrupole precision.⁴ One sees that the positions of the peaks move even more to the left, the peak of the double pole is now at $\epsilon_{\text{DP}} = 10^{-15.6}$ (magenta, dot-dashed line, labelled $X = \text{DP}[\text{qp}]$), of the single poles is at $\epsilon_{\text{SP}} = 10^{-15.2}$ (light blue, dot-dashed, labeled $X = \text{SP}[\text{qp}]$) and of the constant part is that $\epsilon_{\text{C}} = 10^{-13.2}$ (black, dot-dashed, labelled $X = \text{C}[\text{qp}]$). More importantly, out of 100,000 phase space points samples, not a single point has an accuracy worse than 10^{-4} .

We can now examine what happens when the number of external gluons is increased. At double precision we can see from the position of the peaks and the width of the distributions that the accuracy slowly worsens with increasing N . This is due to a slow accumulation of errors when more terms are added together and to the fact that there are potentially more instabilities. However, at quadrupole precision we see no appreciable worsening of the accuracy with increasing N . For $N = 11$ the peak of the double pole is now at $\epsilon_{\text{DP}} = 10^{-15.2}$, of the single poles is at $\epsilon_{\text{SP}} = 10^{-14.8}$ and of the constant part is that $\epsilon_{\text{C}} = 10^{-12.8}$. Again, out of 100,000 phase space points sampled, not a single point has an accuracy worse than 10^{-4} . Up to $N = 11$ (and probably even for more gluons) quadrupole precision is sufficient to guarantee an accuracy needed for any next-to-leading order QCD correction. If higher precision is desired one can choose to evaluate the few phase space points which have insufficient precision using an arbitrary precision packages such as [72], at the cost of higher computation time.

We note that while the plots here presented are for the MHV amplitudes, we performed a similar study for the finite amplitudes ($A_N^{[1]}(+ \cdots +)$, $A_N^{[1]}(- + \cdots +)$) and obtain very similar results. This indicates that the accuracy is essentially independent of the helicities of the external gluons.

For the results shown in the above plots we choose to rerun all events in quadrupole precision to get an overall picture. However, in practice only a small fraction of phase space points require a quadrupole precision treatment (this fraction can be read off the plots in fig. (1) and depends on N and on the target accuracy). Therefore one needs a systematic procedure to decide which events should be re-evaluated in quadrupole precision. One possible way is to verify the accuracy of the single poles results. The analytic single pole result is given in eq. (3.4) for arbitrary number of gluons. Since two-point functions contain single poles, this checks the coefficients of the two-point master integrals as well as the coefficients of the higher point master integrals. In fig. (2) we investigate the correlation between the accuracy of the single pole contribution and the constant part. We plot the relative accuracy of the constant part $\log_{10}(\epsilon_{\text{C}})$ versus the accuracy on the single poles $\log_{10}(\epsilon_{\text{SP}})$ in double precision (left) for $N = 6$ MHV amplitudes when sampling 1,000 phase space points. The high correlation between the accuracy of the constant part and the single pole is evident. In fig. (2) (right) we show the improvement when running the same points in quadrupole precision (note the different scale on the y-axis). This leaves us with

⁴Only the coefficients of the master integrals are computed in quadrupole precision, master integrals are still calculated in double precision.

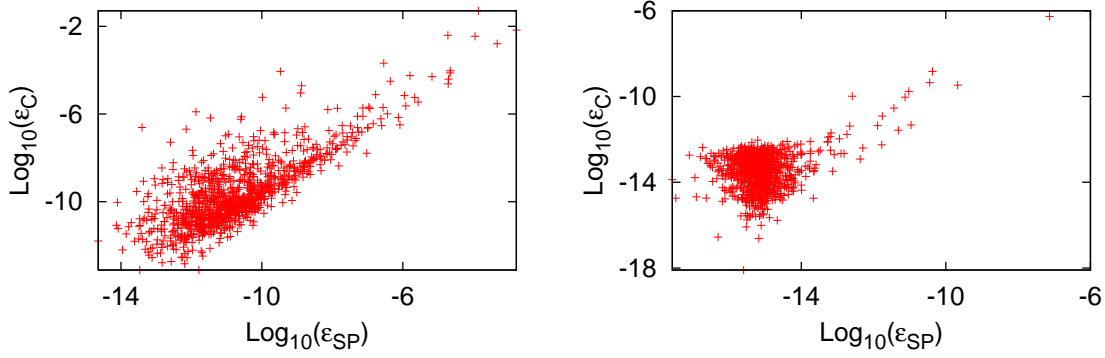


Figure 2: Relative accuracy of the constant part versus the accuracy on the single poles in double precision (left) and quadrupole precision (right) for $N = 6$ MHV amplitudes when sampling 1,000 phase space points.

a straightforward estimate of the accuracy of the one-loop evaluation. By comparing the numerical evaluated single pole result against the analytic single pole result we can decide to switch to quadruple precision to re-evaluate the full one-loop amplitude and get the required precision. Alternatively, one might choose to run in quadrupole precision whenever any small denominator (for instance in the construction of dual vectors) appears. We did not fully investigate yet which method is the most efficient in detecting potential instabilities. We will leave this to a future study, but we anticipate that identifying dangerous phase space points in order to increase the accuracy is not an issue.

3.3 Time Dependence of the Algorithm

Compared to traditional Feynman diagram approaches, the power of this method is that the time needed to compute one-loop amplitudes does not grow factorially with the number of external legs. It is indeed quite straightforward to estimate the scaling of time with the number of gluons N . Within the so-called constructive implementation of Berends-Giele recursion relations (or alternatively a recursive implementation “with memory”) the time required to compute tree level ordered amplitudes grows as $\tau_{\text{tree},N} \propto N^4$ [18]. Altogether the number of tree amplitudes that one needs to evaluate at one-loop is simply given by

$$n_{\text{tree}} = \{(D_{s_1} - 2)^2 + (D_{s_2} - 2)^2\} \times \left(5 c_{5,\text{max}} \binom{N}{5} + 4 c_{4,\text{max}} \binom{N}{4} + 3 c_{3,\text{max}} \binom{N}{3} + 2 c_{2,\text{max}} \left[\binom{N}{2} - N \right] \right), \quad (3.6)$$

where the first factor is due to the sum over polarization of the internal cut gluons in D_{s_1} and D_{s_2} dimensions respectively needed to determine the dimensional dependence of the one-loop amplitude [51]. The constants $c_{m,\text{max}}$ denote the number of times one needs to perform a multiple cut in order to fully constraint the system of equations determining the master integral coefficients. Explicitly we have $c_{5,\text{max}} = 1$, $c_{4,\text{max}} = 5$, $c_{3,\text{max}} = 10$, and $c_{2,\text{max}} = 10$ [51]. The integer number in front counts the number of tree amplitudes per multiple cut, finally the binomial coefficients corresponds to the number of possible

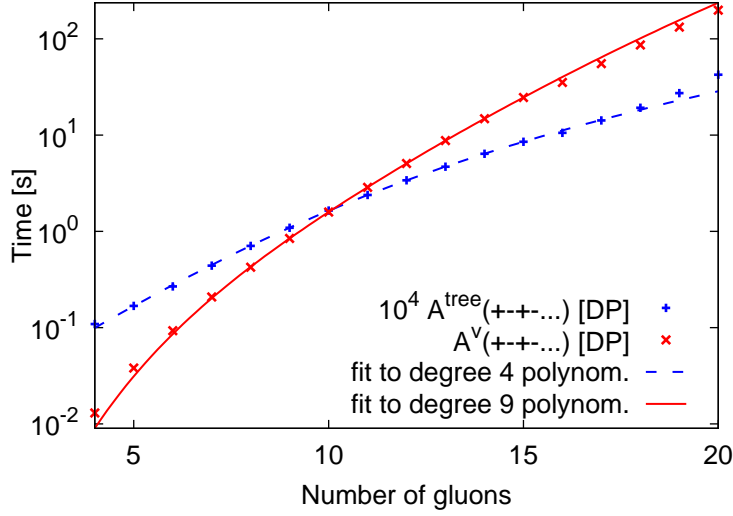


Figure 3: Time in seconds needed to compute tree (blue, dashed) and one-loop (red, solid) ordered amplitudes with gluons of alternating helicity signs, $A_N^{[1]}(+ - + - \dots)$, as a function of the number of external gluons ranging between 4 to 20 using a single 2.33 GHz Xeon processor.

cuts (for two point functions we subtract the vanishing contributions of the external self energy graphs). From this it follows that the time needed to evaluate a one-loop ordered amplitude will for large N scale as

$$\tau_{\text{one-loop},N} \sim n_{\text{tree}} \cdot \tau_{\text{tree},N} \propto N^9. \quad (3.7)$$

In fig. (3) we plot the time needed to compute tree (blue, dashed) and one-loop (red, solid) ordered amplitudes with alternating helicity signs for the gluons, $A_N^{[1]}(+ - + - \dots)$, as a function of the number of gluons in the range between four and twenty. Time estimates refer to using a 2.33 GHz Xeon processor. One can see that the times needed to compute tree and one-loop ordered amplitudes are consistent with a N^4 and N^9 growth respectively (we show a polynomial fit to those points as well).⁵ When running in quadrupole precision rather than in double precision the evaluation time grows with a factor of approximately thirty. We verified that the scaling with N is unchanged.

Finally we remark that the time needed to compute “easier” or more “difficult” helicity amplitudes is approximately the same, i. e. we checked that the plot looks essentially identical for other helicity configurations.

3.4 Results for fixed phase space points

In this section we present sample results for one-loop helicity amplitudes at fixed phase space points for $N = 6, 7$. Other results for N ranging from eight to twenty are given in

⁵The evaluation times given in ref. [54] for 6, 7 and 8 gluon MHV amplitudes make use of analytic expressions for the required tree amplitudes. Nevertheless, the average time for the most complicated 6 gluon helicity amplitudes quoted is 72ms per phase space point, while we have an average computation time of 90ms for any of the helicity amplitude.

Appendix A. Since the algorithm employed is independent of the chosen external helicity vectors we show, apart from a comparison with known amplitudes, the results for the “most difficult”, alternating sign helicity configurations, $A_N^{[1]}(+ - + - \dots)$. (A zero in the tables means results smaller than 10^{-15} .)

$N = 6$ We choose in this case the same phase space point as in [23], i.e. the six momenta p_i are chosen as follows, $p = (E, p_x, p_y, p_z)$,⁶

$$\begin{aligned}
p_1 &= (-3.000000000000000, 1.837117307087384, -2.121320343559642, 1.060660171779821) \\
p_2 &= (-3.000000000000000, -1.837117307087384, 2.121320343559642, -1.060660171779821) \\
p_3 &= (2.000000000000000, 0.000000000000000, -2.000000000000000, 0.000000000000000) \\
p_4 &= (0.857142857142857, 0.000000000000000, 0.315789473684211, 0.796850604480708) \\
p_5 &= (1.000000000000000, 0.866025403784439, 0.184210526315789, 0.464829519280413) \\
p_6 &= (2.142857142857143, -0.866025403784439, 1.500000000000000, -1.261680123761121) .
\end{aligned} \tag{3.8}$$

We obtain the same results as in [23], which we give in Table 1 for completeness.

Helicity amplitude	c_Γ/ϵ^2	c_Γ/ϵ	1
$ A_6^{\text{tree}}(+ + + + +) $	-	-	$1.767767365814634 \cdot 10^{-15}$
$ A_6^{\text{v,unit}}(+ + + + +) $	0	0	0.529806483643855
$ A_6^{\text{v,num}}(+ + + + +) $	$1.060660419488780 \cdot 10^{-14}$	$3.813284749527035 \cdot 10^{-14}$	0.529806483661295
$ A_6^{\text{tree}}(- + + + +) $	-	-	$3.963158957208070 \cdot 10^{-14}$
$ A_6^{\text{v,unit}}(- + + + +) $	$1.011255761241711 \cdot 10^{-11}$	$6.753625348984687 \cdot 10^{-10}$	3.25996704351899
$ A_6^{\text{v,num}}(- + + + +) $	$2.377895374324842 \cdot 10^{-13}$	$8.549005883762705 \cdot 10^{-13}$	3.25996705427236
$ A_6^{\text{tree}}(- - + + +) $	-	-	28.4912816504432
$ A_6^{\text{v,unit}}(- - + + +) $	170.947689902659	614.590878376396	1373.74753500854
$ A_6^{\text{v,num}}(- - + + +) $	170.947689902659	614.590878376397	1373.74753500828
$ A_6^{\text{tree}}(- + - + -) $	-	-	3.13871539500808
$ A_6^{\text{v,unit}}(- + - + -) $	18.8322923700467	67.7058293474830	151.043950328960
$ A_6^{\text{v,num}}(- + - + -) $	18.8322923700485	67.7058292869577	151.043950337947
$ A_6^{\text{tree}}(+ - + - +) $	-	-	3.13871539500808
$ A_6^{\text{v,unit}}(+ - + - +) $	18.8322923700554	67.7058292857048	153.780101529836
$ A_6^{\text{v,num}}(+ - + - +) $	18.8322923700485	67.7058292869577	153.780101415986

Table 1: Results for tree level and one-loop virtual (unrenormalized) amplitudes in the FDH scheme for some helicity configurations for the case of six external gluons for the phase space point of eq. (3.8). Comparison with known results is also shown.

$N = 7$ We randomly choose the following phase space point:

$$\begin{aligned}
p_1 &= (-3.500000000000000, 3.500000000000000, 0.000000000000000, 0.000000000000000) \\
p_2 &= (-3.500000000000000, -3.500000000000000, 0.000000000000000, 0.000000000000000) \\
p_3 &= (1.721020317835363, 0.501455810979379, 0.991016354865482, -1.314663298501285) \\
p_4 &= (2.156731348769508, -1.341260229883955, 1.169853444323893, 1.218176516478751) \\
p_5 &= (1.037618172453970, -0.152260900991984, -0.998573413613423, 0.237316723937150) \\
p_6 &= (0.584066733036484, 0.353785124568635, 0.163503402186405, -0.435013415594666) \\
p_7 &= (1.500563427904675, 0.638280195327925, -1.325799787762357, 0.294183473680051)
\end{aligned} \tag{3.9}$$

The results are given in Table 2.

⁶Note however that we use a different convention to label the momentum components here.

Helicity amplitude	c_Γ/ϵ^2	c_Γ/ϵ	1
$ A_7^{\text{tree}}(+ + + + + +) $	-	-	0
$ A_7^{\text{v,unit}}(+ + + + + +) $	0	$1.256534542409480 \cdot 10^{-10}$	0.310169532972026
$ A_7^{\text{v,anly}}(+ + + + + +) $	0	$1.250170111559883 \cdot 10^{-15}$	0.310169533483183
$ A_7^{\text{tree}}(- + + + + +) $	-	-	0
$ A_7^{\text{v,unit}}(- + + + + +) $	$3.678212874319657 \cdot 10^{-13}$	$7.209572152581734 \cdot 10^{-13}$	0.192052814810810
$ A_7^{\text{v,anly}}(- + + + + +) $	$2.713533399763100 \cdot 10^{-15}$	$8.924875144594874 \cdot 10^{-15}$	0.192052814765395
$ A_7^{\text{tree}}(- - + + + +) $	-	-	2.10661283459449
$ A_7^{\text{v,unit}}(- - + + + +) $	14.7462898421614	48.5008939631214	87.3152155138790
$ A_7^{\text{v,anly}}(- - + + + +) $	14.7462898421614	48.5008939631213	87.3152155138651
$ A_7^{\text{tree}}(- - + - + -) $	-	-	0.110186568094442
$ A_7^{\text{v,unit}}(- - + - + -) $	0.771305976661093	2.53684348996073	5.93361050294547
$ A_7^{\text{v,anly}}(- - + - + -) $	0.771305976661095	2.53684348996075	N.A.
$ A_7^{\text{tree}}(+ - + - + -) $	-	-	0.110186568094442
$ A_7^{\text{v,unit}}(+ - + - + -) $	0.771305976661093	2.53684348996074	6.04201240991614
$ A_7^{\text{v,anly}}(+ - + - + -) $	0.771305976661095	2.53684348996075	N.A.

Table 2: Results for tree level and one-loop virtual (unrenormalized) amplitudes in the FDH scheme for some helicity configurations for the case of seven external gluons for the phase space point of eq. (3.9). Comparison with analytical results, when available, is also shown.

4. Conclusions and outlook

In this paper we present the numerical implementation of an integer dimensional on-shell method for calculating one-loop amplitudes. The method used was developed in refs. [49, 51] which we followed closely. The resulting program, **Rocket**, is a **Fortran** 95 code. The only limitation on the number of external particles are the available computer resources.

As a first example and test of the implemented algorithm we calculated purely gluonic color ordered one-loop amplitudes. We explicitly study the properties and time-behavior of the algorithm up to twenty external gluons. The scaling of the computer time needed to evaluate color ordered one-loop amplitudes is consistent with the theoretical estimate of a rank nine polynomial. Comparisons to existing analytic results for special helicity configuration shows a good numerical accuracy and only for a limited set of events quadrupole precision is required. For completeness and later reference we give numerical results for explicit events.

Now that the algorithm has been validated up to twenty external particles we plan to include internal and external (massive) quarks and external vector bosons. This allows us to compute one-loop amplitudes to a large range of processes relevant for both the LHC and Tevatron experiments.

We envision the collection of one-loop matrix elements to be integrated through matching into parton shower Monte Carlo's. The parton shower Monte Carlo will integrate the one-loop matrix elements with the radiative contributions. This will allow a seamless integration of the available tools in a single framework and will provide a complete and advanced analysis tool for experimentalists.

Acknowledgments

We thank Fabio Maltoni for providing tree level amplitudes for checks and Lance Dixon and Keith Ellis for comments on the manuscript. W.G thanks Jan Winter for useful discussions. G.Z. is supported by the British Science and Technology Facilities Council (STFC). G.Z. would like to thank Mainz University and CERN for hospitality while part of this work was carried out.

A. More numerical results

In this appendix we list some explicit results for high multiplicity events.

$N = 8$ We randomly choose the following phase space point:

$$\begin{aligned}
p_1 &= (-4.000000000000000, 4.000000000000000, 0.000000000000000, 0.000000000000000) \\
p_2 &= (-4.000000000000000, -4.000000000000000, 0.000000000000000, 0.000000000000000) \\
p_3 &= (1.449692512284710, 0.958721567196264, 0.596442789329140, 0.909239977027169) \\
p_4 &= (1.009340416556955, -0.511164560265637, 0.004406444973267, 0.870321464785572) \\
p_5 &= (1.065731003301513, 0.640468049755497, -0.851783840257115, -0.006894789139810) \\
p_6 &= (1.402207989626767, 0.338467194877458, -0.023915684844839, -1.360534911049079) \\
p_7 &= (1.702524230799814, -0.823031265059939, 1.480876536483203, -0.167967189914708) \\
p_8 &= (1.370503847430242, -0.603460986503644, -1.206026245683657, -0.244164551709144) . \quad (\text{A.1})
\end{aligned}$$

The results are given in Table 3.

Helicity amplitude	c_Γ/ϵ^2	c_Γ/ϵ	1
$ A_8^{\text{tree}}(++++++) $	-	-	0
$ A_8^{\text{v,unit}}(++++++) $	0	0	0.196700600695691
$ A_8^{\text{v,analy}}(++++++) $	$3.853462894343397 \cdot 10^{-15}$	$1.441159379540454 \cdot 10^{-14}$	0.196700600738201
$ A_8^{\text{tree}}(-++++++) $	-	-	$2.257277386254959 \cdot 10^{-15}$
$ A_8^{\text{v,unit}}(-++++++) $	0	$1.965638104048654 \cdot 10^{-10}$	0.528774716493063
$ A_8^{\text{v,analy}}(-++++++) $	$1.805821909003967 \cdot 10^{-14}$	$6.753606439965886 \cdot 10^{-14}$	0.528774717652170
$ A_8^{\text{tree}}(- - + + + +) $	-	-	4.33318919466960
$ A_8^{\text{v,unit}}(- - + + + +) $	34.6655135573561	129.645805347145	274.299773434926
$ A_8^{\text{v,analy}}(- - + + + +) $	34.6655135573568	129.645805291409	274.299773434900
$ A_8^{\text{tree}}(- + - + - +) $	-	-	$7.261522613885579 \cdot 10^{-2}$
$ A_8^{\text{v,unit}}(- + - + - +) $	0.580921809110773	2.17259368023597	5.47630381976679
$ A_8^{\text{v,analy}}(- + - + - +) $	0.580921809110846	2.17259368244769	N.A.
$ A_8^{\text{tree}}(+ - + - + -) $	-	-	$7.261522613885579 \cdot 10^{-2}$
$ A_8^{\text{v,unit}}(+ - + - + -) $	0.580921809110862	2.17259368781042	4.92550054630729
$ A_8^{\text{v,analy}}(+ - + - + -) $	0.580921809110846	2.17259368244769	N.A.

Table 3: Results for tree level and one-loop virtual (unrenormalized) amplitudes in the FDH scheme for some helicity configurations for the case of eight external gluons for the phase space point of eq. (A.1). Comparison with analytical results, when available, is also shown.

$N = 9$ We randomly choose the following phase space point:

$$\begin{aligned}
p_1 &= (-4.500000000000000, 4.500000000000000, 0.000000000000000, 0.000000000000000) \\
p_2 &= (-4.500000000000000, -4.500000000000000, 0.000000000000000, 0.000000000000000) \\
p_3 &= (0.837513535184208, -0.699991554911619, -0.341245468610472, 0.308208168000110) \\
p_4 &= (0.173971130750340, -0.127314067058472, -0.036582419646361, 0.112777698311325) \\
p_5 &= (1.527678295320022, -0.329915424080283, -1.066446319295822, -1.042904135098816) \\
p_6 &= (1.087863978393825, -0.427338530001958, -0.959598549771965, 0.282843489474564) \\
p_7 &= (2.837576052736588, 0.906765089674632, 2.135787640996821, -1.633409342380760) \\
p_8 &= (2.065394708000926, 0.474995872769939, 0.683997980573425, 1.890074332734359) \\
p_9 &= (0.470002299614090, 0.202798613607760, -0.415912864245626, 0.082409788959218). \tag{A.2}
\end{aligned}$$

The results are given in Table 4.

Helicity amplitude	c_Γ/ϵ^2	c_Γ/ϵ	1
$ A_9^{\text{tree}}(++++++) $	-	-	$2.992915640032351 \cdot 10^{-14}$
$ A_9^{\text{v,unit}}(++++++) $	$4.860269836292316 \cdot 10^{-12}$	$1.845193695700690 \cdot 10^{-08}$	5.66655561706295
$ A_9^{\text{v,anly}}(++++++) $	$2.693624076029116 \cdot 10^{-13}$	$1.176695244346755 \cdot 10^{-12}$	5.66655558047311
$ A_9^{\text{tree}}(-++++++) $	-	-	$9.114087930248735 \cdot 10^{-14}$
$ A_9^{\text{v,unit}}(-++++++) $	$3.938371378126140 \cdot 10^{-11}$	$2.340429860576292 \cdot 10^{-08}$	1.06208646061428
$ A_9^{\text{v,anly}}(-++++++) $	$8.202679137223861 \cdot 10^{-13}$	$3.583296428617654 \cdot 10^{-12}$	1.06208646798175
$ A_9^{\text{tree}}(--++++++) $	-	-	32.3229667945508
$ A_9^{\text{v,unit}}(--++++++) $	290.906701096922	1270.81033486132	3625.43061670521
$ A_9^{\text{v,anly}}(--++++++) $	290.906701150957	1270.81033630185	3625.43061670594
$ A_9^{\text{tree}}(-+-+--+--) $	-	-	0.453521966367950
$ A_9^{\text{v,unit}}(-+-+--+--) $	4.08169769666186	17.8306776720814	57.1063950462874
$ A_9^{\text{v,anly}}(-+-+--+--) $	4.08169769731155	17.8306776807844	N.A.
$ A_9^{\text{tree}}(+--+--+--+) $	-	-	0.453521966367950
$ A_9^{\text{v,unit}}(+--+--+--+) $	4.08169769662055	17.8306776454842	55.0153807707576
$ A_9^{\text{v,anly}}(+--+--+--+) $	4.08169769731155	17.8306776807844	N.A.

Table 4: Results for tree level and one-loop virtual (unrenormalized) amplitudes in the FDH scheme for some helicity configurations for the case of nine external gluons for the phase space point of eq. (A.2). Comparison with analytical results, when available, is also shown.

$N = 10$ We randomly choose the following phase space point:

$$\begin{aligned}
p_1 &= (-5.000000000000000, 5.000000000000000, 0.000000000000000, 0.000000000000000) \\
p_2 &= (-5.000000000000000, -5.000000000000000, 0.000000000000000, 0.000000000000000) \\
p_3 &= (1.532520310665362, 1.513070043279136, -0.187195319404816, 0.155548896254710) \\
p_4 &= (0.258067002946760, -0.183609750404875, -0.180504757414873, 0.017437606394811) \\
p_5 &= (0.933615908667822, -0.324162340665056, -0.045792611756259, -0.874334305926935) \\
p_6 &= (1.406380992739491, 0.945471671828880, -0.641345241905772, -0.820162846752305) \\
p_7 &= (0.826140594064319, 0.546878011685178, -0.615447980566360, -0.068238586686725) \\
p_8 &= (1.003938368361987, -0.166638867622269, 0.778081660907425, -0.612137782060901) \\
p_9 &= (0.626103283169757, -0.367431900674052, 0.140872898707371, -0.486984543874634) \\
p_{10} &= (3.413233539384504, -1.963576867426942, 0.751331351433283, 2.688871562651979). \tag{A.3}
\end{aligned}$$

The results are given in Table 5.

Helicity amplitude	c_Γ/ϵ^2	c_Γ/ϵ	1
$ A_{10}^{\text{tree}}(++++++) $	-	-	$7.645214091184737 \cdot 10^{-14}$
$ A_{10}^{\text{v,unit}}(++++++) $	$2.616999209810146 \cdot 10^{-13}$	$7.453142378465002 \cdot 10^{-07}$	18.4349011284670
$ A_{10}^{\text{v,anly}}(++++++) $	$7.645214091184737 \cdot 10^{-13}$	$3.853184186191476 \cdot 10^{-12}$	18.4349011284671
$ A_{10}^{\text{tree}}(-++++++) $	-	-	$3.138928592085274 \cdot 10^{-13}$
$ A_{10}^{\text{v,unit}}(-++++++) $	$1.729567134060808 \cdot 10^{-11}$	$3.462486730362966 \cdot 10^{-06}$	14.1180690283674
$ A_{10}^{\text{v,anly}}(-++++++) $	$3.138928592085274 \cdot 10^{-12}$	$1.582018484813023 \cdot 10^{-11}$	14.1180690283692
$ A_{10}^{\text{tree}}(--++++++) $	-	-	489.972695666341
$ A_{10}^{\text{v,unit}}(--++++++) $	4899.72695665607	24694.6000400099	75844.9101458089
$ A_{10}^{\text{v,anly}}(--++++++) $	4899.72695666341	24694.6000476827	75844.9101457814
$ A_{10}^{\text{tree}}(-+-+--+) $	-	-	9.34611372008902
$ A_{10}^{\text{v,unit}}(-+-+--+) $	93.4611371998759	471.043678702711	1481.27447605664
$ A_{10}^{\text{v,anly}}(-+-+--+) $	93.4611372008902	471.043677247939	N.A.
$ A_{10}^{\text{tree}}(+--+--+) $	-	-	9.34611372008902
$ A_{10}^{\text{v,unit}}(+--+--+) $	93.4611371995618	471.043674005742	1503.97025803111
$ A_{10}^{\text{v,anly}}(+--+--+) $	93.4611372008902	471.043677247939	N.A.

Table 5: Results for tree level and one-loop virtual (unrenormalized) amplitudes in the FDH scheme for some helicity configurations for the case of ten external gluons for the phase space point of eq. (A.3). Comparison with analytical results, when available, is also shown.

$N = 15$ We randomly choose the following phase space point:

$$\begin{aligned}
p_1 &= (-7.500000000000000, 7.500000000000000, 0.000000000000000, 0.000000000000000) \\
p_2 &= (-7.500000000000000, -7.500000000000000, 0.000000000000000, 0.000000000000000) \\
p_3 &= (0.368648489648050, 0.161818085189973, 0.125609635286264, -0.306494430207942) \\
p_4 &= (0.985841964092509, -0.052394238926518, -0.664093578996812, 0.726717923425790) \\
p_5 &= (1.470453194926588, -0.203016239158633, 0.901766792550452, -1.143605551298596) \\
p_6 &= (2.467058579094687, -1.840106401193462, 0.715811527707121, 1.479189075734789) \\
p_7 &= (0.566021478235079, -0.406406330753485, -0.393435666409983, -0.020556861225509) \\
p_8 &= (0.419832726637289, -0.214182754609525, 0.074852807863799, -0.353245414886707) \\
p_9 &= (2.691168687878469, 1.868400546247601, 1.850615607221259, -0.571568175905795) \\
p_{10} &= (1.028090983779864, -0.986442664896249, -0.193408556327968, 0.215627155388572) \\
p_{11} &= (1.377779821947130, -0.155359745837053, -1.074009172530291, -0.848908054184264) \\
p_{12} &= (1.432526153404585, 0.621168997409793, -0.290964068761809, 1.257624811911176) \\
p_{13} &= (0.335532948820133, 0.244811479043329, 0.138986808214636, 0.182571538348285) \\
p_{14} &= (1.085581415795683, 0.330868645896313, -0.756382142822373, -0.704910635118478) \\
p_{15} &= (0.771463555739934, 0.630840621587917, -0.435349992994295, 0.087558618018677). \tag{A.4}
\end{aligned}$$

The results are given in Table 6.

Helicity amplitude	c_Γ/ϵ^2	c_Γ/ϵ	1
$ A_{15}^{\text{tree}}(+ + + + \dots) $	-	-	0
$ A_{15}^{\text{v,unit}}(+ + + + \dots) $	0	0	1.07572071884782
$ A_{15}^{\text{v,anly}}(+ + + + \dots) $	0	0	1.07572071880769
$ A_{15}^{\text{tree}}(- + + + \dots +) $	-	-	0
$ A_{15}^{\text{v,unit}}(- + + + \dots +) $	0	0	0.181194659968483
$ A_{15}^{\text{v,anly}}(- + + + \dots +) $	0	0	0.181194659846677
$ A_{15}^{\text{tree}}(- - + + \dots +) $	-	-	7.45782101450887
$ A_{15}^{\text{v,unit}}(- - + + \dots +) $	111.867315217633	586.858955605213	1810.13038312828
$ A_{15}^{\text{v,anly}}(- - + + \dots +) $	111.867315217633	586.858955605213	1810.13038312852
$ A_{15}^{\text{tree}}(- + - \dots +) $	-	-	$5.851039428822597 \cdot 10^{-3}$
$ A_{15}^{\text{v,unit}}(- + - \dots +) $	$8.776559143021942 \cdot 10^{-2}$	0.460420629357800	1.52033417713680
$ A_{15}^{\text{v,anly}}(- + - \dots +) $	$8.776559143233895 \cdot 10^{-2}$	0.460420661976678	N.A.
$ A_{15}^{\text{tree}}(+ - + \dots -) $	-	-	$5.851039428822597 \cdot 10^{-3}$
$ A_{15}^{\text{v,unit}}(+ - + \dots -) $	$8.776559143021942 \cdot 10^{-2}$	0.460420565320471	1.52960647292231
$ A_{15}^{\text{v,anly}}(+ - + \dots -) $	$8.776559143233895 \cdot 10^{-2}$	0.460420661976678	N.A.

Table 6: Results for tree level and one-loop virtual (unrenormalized) amplitudes in the FDH scheme for some helicity configurations for the case of fifteen external gluons for the phase space point of eq. (A.4). Comparison with analytical results, when available, is also shown. The present results have been obtained by running in quadrupole precision.

$N = 20$ We randomly choose the following phase space point:

$$\begin{aligned}
p_1 &= (-10.00000000000000, 10.00000000000000, 0.00000000000000, 0.00000000000000) \\
p_2 &= (-10.00000000000000, -10.00000000000000, 0.00000000000000, 0.00000000000000) \\
p_3 &= (0.325540699096246, -0.312416065575525, 0.033104753113790, 0.085305474968826) \\
p_4 &= (0.848759269032669, -0.024590847182333, -0.848289178399890, 0.013894488596740) \\
p_5 &= (1.570982650317940, 0.440773273547400, 0.720246141672893, -1.324745599853646) \\
p_6 &= (0.553167263468587, -0.230303833105897, -0.480156399163221, -0.149679651832391) \\
p_7 &= (0.503893441998193, -0.080227334603420, -0.333549326254518, 0.369075903611134) \\
p_8 &= (1.342531690799994, -0.248744151369669, 0.500198592589739, 1.220786244980225) \\
p_9 &= (2.116396457930369, 0.026327408340262, -0.849622753763036, -1.938190395961762) \\
p_{10} &= (0.602748352923314, -0.444717464828695, -0.325013925746484, 0.244740477851469) \\
p_{11} &= (1.497270156443179, -1.005250846935450, 0.200161613080160, -1.091432079774134) \\
p_{12} &= (1.403440100824101, 0.989809299131399, 0.670534066899850, -0.735054918411486) \\
p_{13} &= (1.968885859795150, 1.683278410651605, -0.987433952876609, -0.260882176167652) \\
p_{14} &= (0.537434314204394, 0.448194620535905, -0.219499970243363, 0.199441688897247) \\
p_{15} &= (2.339779276321334, -1.532082130972216, 0.290600646542316, 1.744374578491559) \\
p_{16} &= (0.894504093025053, -0.210636900721777, 0.805755963464840, 0.326384735908015) \\
p_{17} &= (0.306394773317926, -0.289150435585858, 0.066148943112216, -0.076773042418471) \\
p_{18} &= (0.560235842911576, -0.343584006920049, 0.286594014336811, 0.337161831792864) \\
p_{19} &= (1.070093313805907, 0.323329544655228, 1.003388464788536, -0.183764236276963) \\
p_{20} &= (1.557942443784069, 0.809991460939089, -0.533167693154030, 1.219356675598426)
\end{aligned}$$

(A.5)

The results are given in Table 7.

Helicity amplitude	c_Γ/ϵ^2	c_Γ/ϵ	1
$ A_{20}^{\text{tree}}(+++...) $	-	-	0
$ A_{20}^{\text{v,unit}}(+++...) $	0	0	1.78947750851720
$ A_{20}^{\text{v,anly}}(+++...) $	0	0	1.789477509283
$ A_{20}^{\text{tree}}(-+++...+) $	-	-	0
$ A_{20}^{\text{v,unit}}(-+++...+) $	0	0	0.303337144522210
$ A_{20}^{\text{v,anly}}(-+++...+) $	0	0	0.303337141901917
$ A_{20}^{\text{tree}}(--++...+) $	-	-	16.7096151501841
$ A_{20}^{\text{v,unit}}(--++...+) $	334.192303003683	1995.15970325579	6882.49682704505
$ A_{20}^{\text{v,anly}}(--++...+) $	334.192303003683	1995.15970325579	6882.49682704481
$ A_{20}^{\text{tree}}(-+-...+) $	-	-	$2.0970621000196 \cdot 10^{-5}$
$ A_{20}^{\text{v,unit}}(-+-...+) $	$4.194124200605681 \cdot 10^{-4}$	$2.503931965487835 \cdot 10^{-3}$	$8.456871985787404 \cdot 10^{-3}$
$ A_{20}^{\text{v,anly}}(-+-...+) $	$4.194124200039273 \cdot 10^{-4}$	$2.503931873702081 \cdot 10^{-3}$	N.A.
$ A_{20}^{\text{tree}}(+--+...+) $	-	-	$2.0970621000196 \cdot 10^{-5}$
$ A_{20}^{\text{v,unit}}(+--+...+) $	$4.194124200605681 \cdot 10^{-4}$	$2.503931902332899 \cdot 10^{-3}$	$9.203156962017870 \cdot 10^{-3}$
$ A_{20}^{\text{v,anly}}(+--+...+) $	$4.194124200039273 \cdot 10^{-4}$	$2.503931873702081 \cdot 10^{-3}$	N.A.

Table 7: Results for tree level and one-loop virtual (unrenormalized) amplitudes in the FDH scheme for some helicity configurations for the case of twenty external gluons for the phase space point of eq. (A.5). Comparison with analytical results, when available, is also shown. The present results have been obtained by running in quadrupole precision.

References

- [1] R. K. Ellis, W. T. Giele and Z. Kunszt, p. 31, contribution to the NLO multileg working group for the Workshop "Physics at TeV Colliders", Les Houches, France, 11-29 June, 2007, Z. Bern *et al.*, arXiv:0803.0494 [hep-ph].
- [2] T. Stelzer and W. F. Long, Comput. Phys. Commun. 81, 357 (1994) [hep-ph/9401258].
- [3] A. Pukhov *et al.*, hep-ph/9908288.
- [4] F. Krauss, R. Kuhn and G. Soff, JHEP 0202, 044 (2002) [hep-ph/0109036].
- [5] G. Belanger, F. Boudjema, J. Fujimoto, T. Ishikawa, T. Kaneko, K. Kato and Y. Shimizu, arXiv:hep-ph/0308080.
- [6] E. Boos *et al.* [CompHEP Collaboration], Nucl. Instrum. Meth. A **534**, 250 (2004) [arXiv:hep-ph/0403113].
- [7] P. de Causmaecker, R. Gastmans, W. Troost and T. T. Wu, Nucl. Phys. B **206**, 53 (1982).
- [8] F. A. Berends, R. Kleiss, P. de Causmaecker, R. Gastmans and T. T. Wu, Nucl. Phys. B **206**, 61 (1982).
- [9] J. F. Gunion and Z. Kunszt, Phys. Lett. **161B** 333 (1985).
- [10] R. Kleiss and W. J. Stirling, Nucl. Phys. B **262** 235 (1985).
- [11] F. A. Berends and W. T. Giele, Nucl. Phys. B **294**, 700 (1987).
- [12] M. L. Mangano, S. J. Parke and Z. Xu, Nucl. Phys. B **298** (1988) 653.
- [13] F. A. Berends and W. T. Giele, Nucl. Phys. B **306**, 759 (1988).
- [14] F. Caravaglios and M. Moretti, Phys. Lett. B 358, 332 (1995) [arXiv:hep-ph/9507237].
- [15] P. Draggiotis, R. H. P. Kleiss and C. G. Papadopoulos, Phys. Lett. B 439, 157 (1998) [arXiv:hep-ph/9807207].
- [16] R. Britto, F. Cachazo and B. Feng, Nucl. Phys. B 715, 499 (2005) [hep-th/0412308].
- [17] R. Britto, F. Cachazo, B. Feng and E. Witten, Phys. Rev. Lett. 94, 181602 (2005) [hep-th/0501052].
- [18] R. Kleiss and H. Kuijf, Nucl. Phys. B **312**, 616 (1989).
- [19] M. L. Mangano, M. Moretti, F. Piccinini, R. Pittau and A. D. Polosa, JHEP 0307, 001 (2003) [hep-ph/0206293].
- [20] A. Kanaki and C. G. Papadopoulos, Comput. Phys. Commun. 132, 306 (2000) [hep-ph/0002082].

- [21] T. Binoth, G. Heinrich, T. Gehrmann and P. Mastrolia, Phys. Lett. B **649** (2007) 422 [arXiv:hep-ph/0703311].
- [22] G. Ossola, C. G. Papadopoulos and R. Pittau, JHEP **0707** (2007) 085 [arXiv:0704.1271 [hep-ph]].
- [23] R. K. Ellis, W. T. Giele and G. Zanderighi, JHEP **0605** (2006) 027 [arXiv:hep-ph/0602185].
- [24] A. Denner, S. Dittmaier, M. Roth and L. H. Wieders, Phys. Lett. B **612**, 223 (2005) [arXiv:hep-ph/0502063].
- [25] A. Denner, S. Dittmaier, M. Roth and L. H. Wieders, Nucl. Phys. B **724**, 247 (2005) [arXiv:hep-ph/0505042].
- [26] Z. Bern, L. J. Dixon, D. C. Dunbar and D. A. Kosower, Nucl. Phys. B **425**, 217 (1994) [hep-ph/9403226].
- [27] Z. Bern and A. G. Morgan, Nucl. Phys. B **467**, 479 (1996) [hep-ph/9511336].
- [28] Z. Bern, L. J. Dixon and D. A. Kosower, Ann. Rev. Nucl. Part. Sci. **46**, 109 (1996) [hep-ph/9602280].
- [29] Z. Bern, L. J. Dixon, D. C. Dunbar and D. A. Kosower, Phys. Lett. B **394**, 105 (1997) [hep-th/9611127].
- [30] R. Britto, F. Cachazo and B. Feng, Nucl. Phys. B **725**, 275 (2005) [hep-th/0412103].
- [31] R. Britto, F. Cachazo and B. Feng, Phys. Rev. D **71**, 025012 (2005) [hep-th/0410179].
- [32] Z. Bern, L. J. Dixon and D. A. Kosower, Phys. Rev. D **71**, 105013 (2005) [hep-th/0501240].
- [33] Z. Bern, L. J. Dixon and D. A. Kosower, Phys. Rev. D **72**, 125003 (2005) [hep-ph/0505055].
- [34] Z. Bern, L. J. Dixon and D. A. Kosower, Phys. Rev. D **73**, 065013 (2006) [hep-ph/0507005].
- [35] C. F. Berger, Z. Bern, L. J. Dixon, D. Forde and D. A. Kosower, Phys. Rev. D **74**, 036009 (2006) [hep-ph/0604195].
- [36] R. Britto, E. Buchbinder, F. Cachazo and B. Feng, Phys. Rev. D **72**, 065012 (2005) [hep-ph/0503132].
- [37] R. Britto, B. Feng and P. Mastrolia, Phys. Rev. D **73**, 105004 (2006) [hep-ph/0602178].
- [38] P. Mastrolia, Phys. Lett. B **644**, 272 (2007) [hep-th/0611091].
- [39] C. Anastasiou, R. Britto, B. Feng, Z. Kunszt and P. Mastrolia, Phys. Lett. B **645**, 213 (2007) [hep-ph/0609191].

- [40] C. Anastasiou, R. Britto, B. Feng, Z. Kunszt and P. Mastrolia, JHEP **0703**, 111 (2007) [hep-ph/0612277].
- [41] R. Britto and B. Feng, Phys. Rev. D **75**, 105006 (2007) [hep-ph/0612089].
- [42] R. Britto and B. Feng, JHEP **0802**, 095 (2008) [0711.4284 [hep-ph]].
- [43] R. Britto, B. Feng and P. Mastrolia, 0803.1989 [hep-ph].
- [44] R. Britto, B. Feng and G. Yang, 0803.3147 [hep-ph].
- [45] D. Forde, Phys. Rev. D **75**, 125019 (2007) [0704.1835 [hep-ph]].
- [46] Z. Bern, L. J. Dixon, D. A. Kosower and S. Weinzierl, Nucl. Phys. B **489**, 3 (1997) [arXiv:hep-ph/9610370].
- [47] Z. Bern, L. J. Dixon and D. A. Kosower, Nucl. Phys. B **513**, 3 (1998) [hep-ph/9708239].
- [48] G. Ossola, C. G. Papadopoulos and R. Pittau, Nucl. Phys. B **763**, 147 (2007) [hep-ph/0609007].
- [49] R. K. Ellis, W. T. Giele and Z. Kunszt, JHEP **0803**, 003 (2008) [0708.2398 [hep-ph]].
- [50] G. Ossola, C. G. Papadopoulos and R. Pittau, JHEP **0803**, 042 (2008) [0711.3596 [hep-ph]].
- [51] W. T. Giele, Z. Kunszt and K. Melnikov, JHEP **0804** (2008) 049 [arXiv:0801.2237 [hep-ph]].
- [52] G. Ossola, C. G. Papadopoulos and R. Pittau, JHEP **0805** (2008) 004 [arXiv:0802.1876 [hep-ph]].
- [53] T. Binoth, G. Ossola, C. G. Papadopoulos and R. Pittau, arXiv:0804.0350 [hep-ph].
- [54] C. F. Berger *et al.*, arXiv:0803.4180 [hep-ph].
- [55] Z. Bern and D. A. Kosower, Nucl. Phys. B **362** (1991) 389.
- [56] G. J. van Oldenborgh and J. A. M. Vermaseren, Z. Phys. C **46**, 425 (1990).
- [57] Z. Bern, A. De Freitas, L. J. Dixon and H. L. Wong, Phys. Rev. D **66** (2002) 085002 [arXiv:hep-ph/0202271].
- [58] Z. Bern and D. A. Kosower, Nucl. Phys. B **379**, 451 (1992).
- [59] G. 't Hooft and M. J. G. Veltman, Nucl. Phys. B **44** (1972) 189.
- [60] Z. Bern, L. J. Dixon, D. C. Dunbar and D. A. Kosower, Nucl. Phys. B **435** (1995) 59 [arXiv:hep-ph/9409265].
- [61] R. K. Ellis and G. Zanderighi, JHEP **0802** (2008) 002 [arXiv:0712.1851 [hep-ph]].

- [62] W. T. Giele and E. W. N. Glover, Phys. Rev. D **46** (1992) 1980.
- [63] Z. Kunszt, A. Signer and Z. Trocsanyi, Nucl. Phys. B **420** (1994) 550 [arXiv:hep-ph/9401294].
- [64] S. Catani, Phys. Lett. B **427** (1998) 161 [arXiv:hep-ph/9802439].
- [65] G. Mahlon, Phys. Rev. D **49**, 4438 (1994) [arXiv:hep-ph/9312276].
- [66] D. Forde and D. A. Kosower, Phys. Rev. D **73** (2006) 061701 [arXiv:hep-ph/0509358].
- [67] R. Kleiss, W. J. Stirling and S. D. Ellis, Comput. Phys. Commun. **40** (1986) 359.
- [68] W. Giele, E. W. N. Glover and G. Zanderighi, Nucl. Phys. Proc. Suppl. **135** (2004) 275 [arXiv:hep-ph/0407016].
- [69] R. K. Ellis, W. T. Giele and G. Zanderighi, Phys. Rev. D **73**, 014027 (2006) [arXiv:hep-ph/0508308].
- [70] A. Denner and S. Dittmaier, Nucl. Phys. B **734**, 62 (2006) [arXiv:hep-ph/0509141].
- [71] V. Del Duca, W. Kilgore, C. Oleari, C. Schmidt and D. Zeppenfeld, Nucl. Phys. B **616** (2001) 367 [arXiv:hep-ph/0108030].
- [72] David H. Bailey, Yozo Hida, Xiaoye S. Li and Brandon Thompson, "ARPREC: An Arbitrary Precision Computation Package," Sept 2002; LBNL-53651.